Vortices in relativistic electron beams

D. Jovanović*

Institute of Physics, P.O. Box 57, Yu-11001 Belgrade, Yugoslavia
and International Centre for Theoretical Physics, P.O. Box 586, I-34100 Trieste, Italy

R. Fedele†

Dipartimento di Scienze Fisiche, Universitá di Napoli and INFN Sezione di Napoli, Complesso Universitario di M. S. Angelo,
via Cintia, I-80126 Napoli, Italy

P. K. Shukla‡

Institut für Theoretische Physik IV, Ruhr–Universität Bochum, D-44780 Bochum, Germany

We demonstrate that a relativistic electron beam is properly described in the moving frame by the electron-magnetohydrodynamic equations of plasma physics. For large beam currents, the accelerator magnetic field is expected to be unstable to the fast magnetic reconnection. We present a plausible saturated state of the fast reconnection, in the form of a complex vortex pattern. The nonlinear dispersion equations of the vortex are derived and the relationship between the vortex structure and the background magnetic field is discussed.

PACS number(s): 29.27.Bd, 41.75.Ht, 52.35.Py, 52.35.Mw

I. INTRODUCTION

Relativistic non-neutral particle beams with high intensities are of broad interest in present day physics and engineering. Their applications range from experiments in high-energy physics and pumping of free-electron lasers and masers by electron beams to inertial confinement fusion by light ion beams, and production of tritium, transmutation of nuclear waste, and production of short-lived isotopes for use in medicine by heavy ion beams. In all the applications, a high beam intensity (or a large electric current) is desirable in order to have a higher yield in the nuclear and other reactions in which the beam is involved. With increase of the beam current, the collective interactions within the beam gain in importance, and thus highly intensive beams behave predominantly as a continuous medium, rather than a collection of individual particles. The collective interaction is realized via the self-consistent fields produced by the beam space charges and currents. For a review of the early results on the self-consistent evolution of the beam distribution function and the electric and magnetic fields, with the use of the Vlasov-Maxwell system of equations, see Ref. [1] and references therein. Recent experiments with debunched beams [2] also revealed a number of kinetic collective phenomena in the beam behavior, which are known in plasma physics, such as plasma echo, etc. A fluid description has been utilized in the study of relativistic beam phenomena, such as electromagnetic filamentation [3] and intense equilibrium flow [4]. A warm-fluid study of ion beam stability is described in Ref [5].

In the case of ion beams, the collective interactions arise

predominantly from density perturbations, i.e., from space charge and finite thermal pressure effects. Due to the large ion mass for beam currents that are technically realizable at the present time, the collisionless skin depth d_i ($d_i = c/\omega_{p,i}$) is several orders of magnitude larger than the beam radius. As a consequence, the magnetic phenomena connected with torsion of the magnetic flux tubes (such as the generation of diamagnetic vortices, magnetic field reconnection, etc.) are, for the ion beams, of small significance. However, magnetic phenomena of this type may develop in large intensity electron beams, whose radius may be close (within an order of magnitude) to the electron collisionless skin depth d_e, where $d_e = c/\omega_{p,e}$. As examples, we mention the future 5 TeV collider [6], designed to operate with particle bunches that are 100 μm long and with 3 μm radius, containing 4×10^8 particles; the density of such a bunched beam is 10^{17} cm^{-3}, corresponding to the electron collisionless skin depth $d_e = 15.35$ μm. The Dutch free-electron maser [7] is energized with an electron beam whose current is 12 A, which corresponds to $r/d_e = 1/20$. Furthermore, diamagnetic electron vortices at the collisionless skin depth scale are known to arise in inductive accelerators [8], where they are responsible for the emergence of unsteady electron flows, and for the turbulent mixing of the electron flows in the beam. However, a stability study of electron beams that would include magnetic effects in realistic geometries, such as fast reconnection, has not yet been developed.

In this paper we investigate some aspects of the perpendicular dynamics of high-intensity electron beams whose radius is comparable with the corresponding collisionless skin depth. Adopting the thermal equilibrium model for the particle distribution [9], we regard the electron beam as a perfectly conductive, warm fluid. Since the space charge of the beam is almost fully neutralized by the effects of the self-magnetic field for relativistic beam velocities, the electron fluid behaves as a quasineutral plasma. On the spatial and

*Email address: djovanov@phy.bg.ac.yu
†Email address: renato.fedele@na.infn.it
‡Email address: ps@tp4.ruhr-uni-bochum.de

temporal scales of interest, it is described by the electron-magnetohydrodynamic (EMHD) equations [10,11].

The magnetic field in an electron accelerator typically has a very complex geometry, whose possible role is to support the beam and provide its focusing in the perpendicular direction. However, such complex magnetic geometries, containing magnetic separatrices and null and X points, are known to be unstable in conductive fluids, such as plasmas. Magnetic field reconnection, which occurs in the presence of magnetic shear and/or the X points, is a well known phenomenon, existing in both collisional and highly collisionless plasmas, such as that in the Earth's magnetotail. X lines are localized singularities of the magnetic field that arise at the intersection of two separatrix surfaces. In fusion machines with divertor chambers they are introduced by the appropriate design of external magnetic coils, but they also evolve self-consistently in the space between neighboring magnetic islands in the course of development of the tearing instability. The propagation of linear waves in the vicinity of X lines in the MHD regime was studied in [12,13]. In the EMHD regime [14,15] a similar behavior of small amplitude perturbations was found, while in the strongly nonlinear regime a self-similar magnetic collapse was anticipated. Similar instabilities are expected to develop in EMHD relativistic electron beams also, described by our Eqs. (16) and (17) (see below).

We demonstrate that a feasible saturated state in the reconnection of the quadrupolar and octupolar components of the magnetic field in an electron beam has the form of an octupolar vortex pattern in the velocity field of the electrons. As such a pattern introduces new bifurcations, with finer scales, in the magnetic field topology, one might expect that this branching process would continue, multiplying the number of vortices with diminishing scale size, eventually leading to stochasticity of the beam (or parts of it). The stochasticity would occur in the vicinity of the original linearly unstable critical points.

II. BASIC EQUATIONS

We study the nonlinear dynamics of a relativistic electron beam. The beam consists of particles whose rest mass and charge are equal to m_e and $-e$, respectively, and which are propagating in the direction of the z axis with a velocity $\vec{e}_z V$ that is highly relativistic ($V \approx c$). The velocity of an individual electron may deviate from the average beam velocity by a relatively small, nonrelativistic, amount. For simplicity, we consider a linear accelerator with a debunched beam, i.e., we assume that the beam is an infinitely long cylinder with radius r_b, placed inside a conductive (metallic) tube whose inner radius is r_w, satisfying $r_w \gg r_b$. The unperturbed beam number density n_0 is assumed to be constant both longitudinally and transversely. The beam is immersed in the magnetic field $\vec{B}$, which can be expressed as

$$\vec{B} = \vec{B}_{\text{ext}} + \vec{B}_{\text{beam}}, \qquad (1)$$

where the magnetic field $\vec{B}_{\text{ext}}$ is produced by the currents in the magnetic coils and in the cylindrical metallic vessel that encloses the vacuum chamber of the accelerator, and $\vec{B}_{\text{beam}}$ is produced by the electric current of the electron beam.

It is convenient to expand the total magnetic field into cylindrical harmonics,

$$\vec{B}(\vec{r},t) = \sum_n \vec{B}_n(r,z,t)\cos(n\theta + \varphi_n), \qquad (2)$$

and we restrict our analysis only to the main contributions in the expansion. In a linear accelerator, the external magnetic field must not possess a dipolar ($n=1$) component, which in circular (ring) machines is used for beam bending. We assume that the largest amplitude in the $\vec{B}_{\text{ext}}$ expansion is that of the quadrupole ($n=2$), which is used for beam focusing. As the Lorentz force associated with the quadrupolar magnetic field produces both beam pinching and stretching (focusing and defocusing) in two mutually perpendicular directions, the magnetic lenses must be periodic along the beam in order to prevent its destruction. The focusing is provided by the average Lorentz force on the particles. We will also account for small monopolar and octupolar components of the total magnetic field, which we assume to be homogeneous in the direction of beam propagation. A monopolar Biot-Savart field is produced self-consistently by the beam current, while the octupolar component has two origins. A part of it is externally applied to achieve the fine tuning of the magnetic lenses, and another part arises accidentally, from small errors in the quadrupolar coils. More details of the magnetic field geometry will be given later.

A. Equations in the beam reference frame

We study the evolution of the electron beam in the comoving reference frame, which is described by the standard Lorentz transformations

$$t' = \left(t - \frac{Vz}{c^2}\right)\left(1 - \frac{V^2}{c^2}\right)^{-1/2}, \quad z' = (z - Vt)\left(1 - \frac{V^2}{c^2}\right)^{-1/2},$$

$$\vec{E}'_\perp = (\vec{E}_\perp + \vec{e}_z V \times \vec{B}_\perp)\left(1 - \frac{V^2}{c^2}\right)^{-1/2},$$

$$\vec{B}'_\perp = \left(\vec{B}_\perp - \vec{e}_z \frac{V}{c^2} \times \vec{E}_\perp\right)\left(1 - \frac{V^2}{c^2}\right)^{-1/2}, \qquad (3)$$

where the primes denote the quantities in the moving frame. Correspondingly, the charge density ρ and the parallel current density j_z are transformed as

$$\rho' = \left(\rho - \frac{V}{c^2} j_z\right)\left(1 - \frac{V^2}{c^2}\right)^{-1/2},$$

$$j'_z = (j_z - \rho V)\left(1 - \frac{V^2}{c^2}\right)^{-1/2}, \qquad (4)$$

while the other physical quantities are not transformed as one goes from the laboratory to the moving frame,

$$x' = x, \quad y' = y, \quad E'_z = E_z, \quad B'_z = B_z, \quad \vec{j}'_\perp = \vec{j}_\perp. \quad (5)$$

Equations (4) are further simplified using $\vec{j}=\rho\vec{v}$, where $\vec{v}$ is the hydrodynamic velocity of the beam. For a highly relativistic beam with a small parallel velocity spread,

$$|v_z-V|\ll|c-V|\ll c,$$

the charge density and the parallel current in the moving frame are negligibly small,

$$\frac{\rho'}{\rho}\sim\frac{j'_z}{j_z}\sim\frac{v_z-V}{c-V}\ll1. \tag{6}$$

Following [5] we adopt the model of a warm fluid that is in thermodynamic equilibrium, neglecting the particle diffusion due to collisions and turbulent effects. Thus, the pressure tensor is taken to be anisotropic but purely diagonal, $\hat{p}=nT_\perp(\vec{e}_x\vec{e}_x+\vec{e}_y\vec{e}_y)+nT_\parallel\vec{e}_z\vec{e}_z$. We also assume small, non-relativistic, deviations of the particle velocities from the average beam velocity $\vec{e}_zV$. Thus, the electron beam dynamics is described by the hydrodynamic momentum equation in the moving frame

$$\left(\frac{\partial}{\partial t'}+\vec{v}'\vec{\nabla}'\right)\vec{v}'=-\frac{e}{m_e}\left(\vec{E}'+\vec{v}'\times\vec{B}'+\frac{\vec{\nabla}'\hat{p}'}{n'e}\right), \tag{7}$$

where the effective pressure $\hat{p}'$ models the beam defocusing by the particle thermal motion, but accounts also for other stochastic processes, including turbulent and quantum effects, etc. Equation (7) will be studied for a debunched coasting beam, with a negligible velocity spread $|v_z-V|\to0$ in the unperturbed state.

B. The separation of time scales

A quadrupolar magnetic field that is periodic along the z axis,

$$\vec{B}_2=\vec{B}_{2,0}(r)\cos2\theta\cos kz, \tag{8}$$

is observed in the moving frame as an electromagnetic wave, whose electric field is equal to

$$\vec{E}'_2=\vec{e}_zV\times\vec{B}'_{2,0}(r')\cos2\theta'\cos(\omega't'+k'z'), \tag{9}$$

where $\vec{B}'_{2,0}(r')=\vec{B}_{2,0}(r)(1-V^2/c^2)^{-1/2}$, $k'=k(1-V^2/c^2)^{-1/2}$, $\omega'=k'V$, $r'=r$, and $\theta'=\theta$. Note that for relativistic velocities we have $k'\gg k$. We will conveniently separate the high- and low-frequency components of the momentum equation (7). As the amplitude of the ''rapid'' component is much larger than that of the ''slow'' one, by performing the average over the rapid oscillations we readily obtain the following slow momentum equation:

$$\left(\frac{\partial}{\partial t'}+\vec{v}'_s\vec{\nabla}'\right)\vec{v}'_s=-\frac{e}{m_e}\left(\vec{E}'_s+\vec{v}'_s\times\vec{B}'_s+\frac{\vec{\nabla}'p'_{,s}}{n'e}-\vec{\nabla}'\phi'_p\right). \tag{10}$$

The subscript s is used to denote the slow components. The last term on the right-hand side of Eq. (11) is the ponderomotive potential ϕ'_p, which is the leading nonlinear term

arising from the coupling with the rapid fields. With accuracy to the leading order, we calculate ϕ'_p using the following solution of the linearized rapid momentum equation:

$$\vec{v}'_r=-\frac{e}{m_ek'}\vec{e}_z\times\vec{B}_{2,0}(r'_0)\cos2\theta'\sin(\omega't+k'z'),$$

where we assumed that the electric field $\vec{E}'_2$, Eq. (9), is the only high-frequency field present in the system. The corresponding ponderomotive potential is then given by

$$\phi'_p\equiv-\frac{m_e}{2e}\langle\vec{v}'^2_r\rangle=-\frac{e}{8m_ek'^2}|\vec{B}'_{2,0_\perp}(r')|^2(1+\cos4\theta'). \tag{11}$$

The ponderomotive force $(e/m)\vec{\nabla}\phi'_p$ represents the average focusing strength of an alternating-gradient lattice of magnetic quadrupoles, discussed in [1,5].

Obviously, in order to avoid solutions of the slow equation (10) that are secularly growing in time (and thus cannot be regarded as slow), the leading order curl-free term on the right-hand side must be identically equal to zero,

$$\phi^{(0)'}_s-\frac{p^{(0)'}_{\perp,s}}{en'}+\phi'_p=0. \tag{12}$$

This expression describes the leading-order hydrodynamic stability of the electron beam.

The leading-order slow potential $\phi^{(0)'}_s$, using Eqs. (3) and (4), can be expressed as

$$\phi^{(0)'}_s=\phi^{(0)'}_{\text{beam}}-VA^{(0)'}_{s,z_{\text{ext}}}, \tag{13}$$

where $\phi^{(0)'}_{\text{beam}}$, in accordance with Eq. (4), is determined from

$$\vec{\nabla}'^2_\perp\phi^{(0)'}_{\text{beam}}=\frac{en}{\epsilon_0}\left(1-\frac{Vv_z}{c^2}\right)\left(1-\frac{V^2}{c^2}\right)^{-1/2},$$

and $A^{(0)'}_{s,z_{\text{ext}}}$ is the z component of the slow vector potential that is associated with external currents (i.e., those in the magnetic coils and the metallic tube). Here we used the fact that the slow magnetic field is strictly two dimensional (i.e., homogeneous in the direction of beam propagation) and thus can be expressed as

$$\vec{B}'_s=\vec{e}_zB'_{s,z}-\vec{e}_z\times\vec{\nabla}'_\perp A'_{s,z}. \tag{14}$$

The condition (12) can be met by the appropriate shaping of the magnetic coils. Technically, this is performed in two stages. First, the quadrupolar magnets are designed so that the monopolar component of the ponderomotive potential produces an *inward* force that fully balances the beam defocusing due to the residual space charge and other effects, discussed earlier. Such an inward ponderomotive force can be produced by the wiggler quadrupolar magnetic field (8) if its amplitude has a minimum at the beam axis ($r=0$). However, such a magnetic field inevitably also produces an octupolar component of the ponderomotive potential [see Eq.

(11)], which is then in the second design stage balanced by the fine tuning of the octupole magnets.

For phase velocities that are much smaller than the speed of light, $|(\partial^2/\partial t^2)\vec{B}'_s| \ll c^2|\vec{\nabla}'^2_\perp\vec{B}'_s|$, we can neglect the displacement current on the slow time scale, and use $\vec{v}'_s = -[c^2\epsilon_0/(n'e)] (\vec{\nabla}' \times \vec{B}'_s)$, while for $d/dt \ll \omega_{p,e} [\omega^2_{p,e} = n'e^2/(m_e\epsilon_0)]$ the beam density may be regarded as negligible. Then, calculating the curl of Eq. (10), we readily obtain the following equation for the slow time evolution of the magnetic field:

$$\frac{\partial}{\partial t'}(1-d_e^2\vec{\nabla}'^2)\vec{B}'_s - \frac{e}{m_e}d_e^2\vec{\nabla}'\times[(\vec{\nabla}'\times\vec{B}'_s)$$

$$\times(1-d_e^2\vec{\nabla}'^2)\vec{B}'_s]=0, \qquad (15)$$

where $d_e=[c^2\epsilon_0 m_e/(n'e^2)]^{1/2}$ is the electron collisionless skin depth.

Equation (15) is identical to the electron-magnetohydrodynamic equations [10], which describe the fast phenomena (compared to the typical ion response time) involving the electron population in collisionless magnetized quasineutral plasmas. In plasma physics, these equations apply to phenomena occurring on spatial scales shorter than the ion skin depth $d_i \equiv c/\omega_{pi}$ and in the frequency range that lies both between the electron and ion gyrofrequencies and below the electron plasma frequency. In other words, EMHD is the regime where the ions are immobile, while both the charge separation and the displacement current are negligible. In our case, the role of the ions is played by the magnetic field of the beam, since for relativistic velocities V the Lorentz force associated with it almost fully compensates for the space charge effects [see Eqs. (4) and (6)] and the beam behaves as if neutralized.

Using the two-dimensionality of the slow magnetic field and Eq. (14), we can rewrite Eq. (15) as a system of two coupled scalar equations (for details, see, e.g., Ref. [15] and references therein)

$$\left(\frac{\partial}{\partial t}+(\vec{e}_z\times\vec{\nabla}_\perp B_z)\cdot\vec{\nabla}_\perp\right)(1-\vec{\nabla}^2_\perp)B_z$$

$$-(\vec{e}_z\times\vec{\nabla}_\perp A_z)\cdot\vec{\nabla}(1-\vec{\nabla}^2_\perp)A_z=0, \qquad (16)$$

$$\left(\frac{\partial}{\partial t}+(\vec{e}_z\times\vec{\nabla}_\perp B_z)\cdot\vec{\nabla}_\perp\right)(1-\vec{\nabla}^2_\perp)A_z=f(t), \qquad (17)$$

where the magnetic field is normalized to an arbitrary field B_0, $\vec{B}\rightarrow\vec{B}'/B_0$, time to the corresponding electron gyroperiod $t\rightarrow-t'eB_0/m_e$, distance to the collisionless skin depth, $\vec{r}\rightarrow\vec{r}'/d_e$, and $f(t)$ is an arbitrary function of time.

C. Stationary solution

For a stationary solution, the arbitrary function $f(t)$ in Eq. (17) must be set to zero. Using $\partial/\partial t=0$, i.e., assuming the

functions A_z and B_z to be dependent only on x and y, Eqs. (15) and (17) take the forms of complete mixed products, and are readily integrated as

$$(1-\vec{\nabla}^2_\perp)A_z=\mathcal{F}(B_z), \qquad (18)$$

$$(1-\vec{\nabla}^2_\perp)B_z+A_z\frac{d\mathcal{F}(B_z)}{dB_z}=\mathcal{G}(B_z). \qquad (19)$$

Here $\mathcal{F}$ and $\mathcal{G}$ are arbitrary functions of the given argument, which in each particular case are to be determined from the appropriate boundary and continuity conditions.

III. OCTUPOLAR VORTEX

Multipolar vortices are characteristic for plasmas that in the unperturbed state feature both velocity and magnetic shears (see Refs. [16–18]). Since in the EMHD plasma regime the parallel magnetic field has the role of a perpendicular stream function, multipoles are expected to arise when the perpendicular and parallel components of the unperturbed magnetic field are nonlinear functions of r and contain higher harmonics in θ. However, such fields inevitably contain also magnetic separatrices and X points, which are known to be unstable.

In this section, we seek a stationary solution (with $\partial/\partial t=0$) in the magnetic configuration that provides the leading-order hydrodynamic beam stability in both its monopolar and octupolar components, as discussed in Sec. II. As a simple model, which satisfies the necessary stability conditions described by Eq. (12), we adopt the background magnetic field in the form

$$B_z^{(0)}=D+\frac{1}{4L_z}(r^2+sr^4\cos 4\theta), \qquad (20)$$

$$A_z^{(0)}=-\frac{1}{4L_\perp}(r^2+sr^4\cos 4\theta), \qquad (21)$$

where D is the (normalized) uniform solenoidal focusing magnetic field, L_z and $L_\perp$ are the characteristic lengths of inhomogeneities in the parallel and perpendicular directions, respectively, and the parameter s determines the amplitude of the octupolar component. The magnetic field (21) possesses an X line in the perpendicular magnetic field at $r=0$, while the parallel magnetic field is adopted so as to have the same separatrix surfaces. Similar magnetic structures were shown to be subject to the fast magnetic reconnection instability in the plasma EMHD regime [14], where it manifested itself either by the formation of magnetic islands in the process of magnetic field merging in a current sheet, or as the formation of singularities near magnetic field separatrices in the course of propagation of small-amplitude whistler waves, or as the formation of singularities in the electron flow near the three-dimensional zero points.

In order to construct the octupole, we solve our basic equations (18) and (19) assuming linear functions $\mathcal{F}$ and $\mathcal{G}$,

$$\mathcal{F}(\xi)=F_0+F_1\xi, \quad \mathcal{G}(\xi)=G_0+G_1\xi, \qquad (22)$$

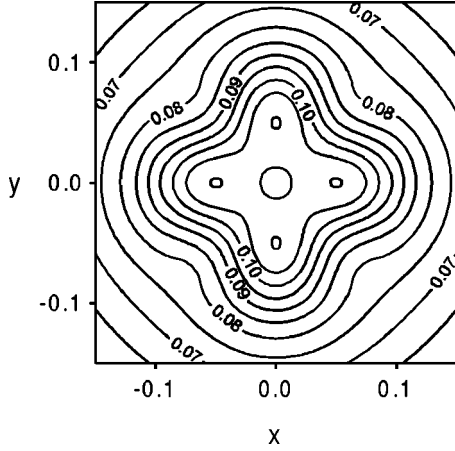FIG. 1. The perturbation of the z component of the vector potential δA_z, associated with the octupole at the axis of an electron beam. The background magnetic field satisfies $L_\perp=1$, $L_z=0.9\,r_0$, $s=2.5/r_0^2$, and the core radius adopted is $r_0=0.1$.

allowing for different values of the parameters inside and outside the vortex core, which is a circle in the x,y plane with the radius r_0.

(1) In the external region $r \geq r_0$ for a solution which is finite for $r \to \infty$ we obviously have

$$F_0^{out}=\frac{1-D}{L_\perp}, \quad G_0^{out}=-\frac{1}{L_z}-D\frac{L_z^2}{L_\perp^2},$$

$$F_1^{out}=\frac{L_z}{L_\perp}, \quad G_1^{out}=1+\frac{L_z^2}{L_\perp^2}, \tag{23}$$

(2) Inside the vortex core $r<r_0$, using linear functions $\mathcal{F}$ and $\mathcal{G}$, Eqs. (18) and (19) may be decoupled to give a linear wave equation of the fourth order,

$$(\vec{\nabla}_\perp^2+\kappa_1^2)(\vec{\nabla}_\perp^2+\kappa_2^2)(A_z^{in}+b)=0. \tag{24}$$

The wave numbers κ_1 and κ_2 are related to the slopes F_1^{in} and G_1^{in} via

$$\kappa_1^2\kappa_2^2=F_1^{in2}+1-G_1^{in}, \quad \kappa_1^2+\kappa_2^2=G_1^{in}-2, \tag{25}$$

and

$$b=-\frac{1}{\kappa_1^2\kappa_2^2}[F_0^{in}(1-G_1^{in})+F_1^{in}G_0^{in}]. \tag{26}$$

Noting that, due to the explicit presence of the terms r^2 and $r^4\cos 4\theta$ in the unperturbed fields $A_z^{(0)}, B_z^{(0)}$, the perturbed fields must also involve the zeroth and fourth cylindrical harmonics,

$$\delta A_z \equiv A_z-A_z^{(0)}=\delta A_{z,0}+\delta A_{z,4}\cos 4\theta,$$

$$\delta B_z \equiv B_z-B_z^{(0)}=\delta B_{z,0}+\delta B_{z,4}\cos 4\theta, \tag{27}$$

and using Eq. (23), we can readily write the solution that is applicable for $r>r_0$. Its zeroth cylindrical harmonic is given by
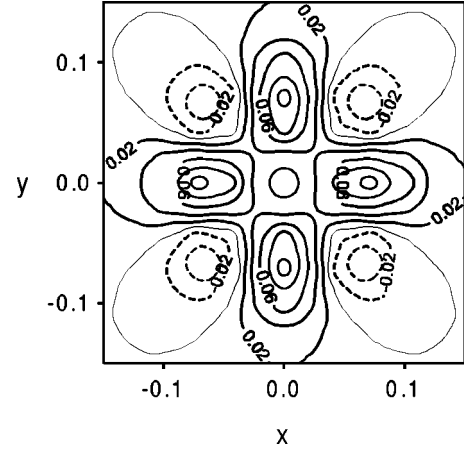

FIG. 2. The parallel magnetic field δB_z of an octupole. The parameters are the same as in Fig. 1.

$$\delta A_{z,0}^{out}=\beta_{0,1}K_0(\rho_1 r), \quad \rho_1=\left(1-\frac{L_z^2}{L_\perp^2}\right)^{1/2},$$

$$\delta B_{z,0}^{out}=-\frac{L_\perp}{L_z}(1-\rho_1^2)\beta_{0,1}K_0(\rho_1 r), \tag{28}$$

while the fourth cylindrical harmonic is equal to

$$\delta A_{z,4}^{out}=\beta_{4,1}K_4(\rho_1 r)+\frac{\beta_{4,2}}{r^4},$$

$$\delta B_{z,4}^{out}=-\frac{L_\perp}{L_z}\left((1-\rho_1^2)\beta_{4,1}K_4(\rho_1 r)+\frac{\beta_{4,2}}{r^4}\right). \tag{29}$$

Likewise, for $r<r_0$ we have

$$\delta A_{z,0}^{in}=\frac{r^2}{4L_\perp}-b+\alpha_{0,1}J_0(\kappa_1 r)+\alpha_{0,2}J_0(\kappa_2 r),$$

$$\delta B_{z,0}^{in}=-\frac{r^2}{4L_z}+\frac{1}{F_1^{in}}[-b-F_0^{in}+(1+\kappa_1^2)\alpha_{0,1}J_0(\kappa_1 r)$$

$$+(1+\kappa_2^2)\alpha_{0,2}J_0(\kappa_2 r)], \tag{30}$$

and

$$\delta A_{z,4}^{in}=\frac{sr^4}{4L_\perp}+\alpha_{4,1}J_4(\kappa_1 r)+\alpha_{4,2}J_4(\kappa_2 r),$$

$$\delta B_{z,4}^{in}=-\frac{sr^4}{4L_z}+\frac{1}{F_1^{in}}[(1+\kappa_1^2)\alpha_{4,1}J_4(\kappa_1 r)$$

$$+(1+\kappa_2^2)\alpha_{4,2}J_4(\kappa_2 r)]. \tag{31}$$

This kind of solution is possible also if one of the "inside" wave numbers is imaginary, e.g., for $\kappa_2^2<0$, when the Bessel function $J_i(\kappa_2 r)$ should be substituted by $I_i(|\kappa_2|r)$, $i=0,4$.

At the edge of the vortex core $r = r_0$, the usual continuity conditions must be satisfied for each cylindrical harmonic. We require that the functions $\mathcal{F}$ and $\mathcal{G}$ are continuous,

$$F_0^{in} + F_1^{in} a = F_0^{out} + F_1^{out} a,$$

$$G_0^{in} + G_1^{in} a = G_0^{out} + G_1^{out} a, \tag{32}$$

that the core edge is an isoline of B_z with the value a,

$$\delta B_{z,0}^{in}(r_0) + \frac{r_0^2}{4L_z} = \delta B_{z,0}^{out}(r_0) + \frac{r_0^2}{4L_z} = a,$$

$$\delta B_{z,4}^{in}(r_0) + \frac{sr_0^4}{4L_z} = \delta B_{z,4}^{out}(r_0) + \frac{sr_0^4}{4L_z} = 0, \tag{33}$$

and that the functions δA_z, $(\partial/\partial r)\delta A_z$, and $(\partial/\partial r)\delta B_z$ are continuous,

$$\delta A_{z,i}^{in}(r_0) = \delta A_{z,i}^{out}(r_0),$$

$$\frac{\partial}{\partial r_0} \delta A_{z,i}^{in}(r_0) = \frac{\partial}{\partial r_0} \delta A_{z,i}^{out}(r_0), \tag{34}$$

$$\frac{\partial}{\partial r_0} \delta B_{z,i}^{in}(r_0) = \frac{\partial}{\partial r_0} \delta B_{z,i}^{out}(r_0), \quad i = 0, 4.$$

Eliminating the constants of integration a, F_0^{in}, G_0^{in}, $\beta_{0,1}$, $\alpha_{0,1}$, and $\alpha_{0,2}$, as well as $\beta_{4,1}$, $\beta_{4,2}$, $\alpha_{4,1}$, and $\alpha_{4,2}$ from Eqs. (32)–(34), we obtain the nonlinear dispersion relation in the form

$$\mathcal{D}_0(\kappa_1, \kappa_2) \equiv \begin{vmatrix} (1 - c\kappa_1^2)\mathcal{J}_{0,1} & (1 - c\kappa_2^2)\mathcal{J}_{0,2} & (c - d)\rho_1^2 \mathcal{K}_{0,1} \\ 2\mathcal{J}_{0,1} + r_0\kappa_1^2\mathcal{J}_{0,1} & 2\mathcal{J}_{0,2} + r_0\kappa_2^2\mathcal{J}_{0,2} & 2\mathcal{K}_{0,1}' - r_0\rho_1^2\mathcal{K}_{0,1} \\ \left(1 + \frac{L_z}{L_\perp}\frac{1+\kappa_1^2}{1+F_1^{in}}\right)\mathcal{J}_{0,1}' & \left(1 + \frac{L_z}{L_\perp}\frac{1+\kappa_2^2}{1+F_1^{in}}\right)\mathcal{J}_{0,2}' & \rho_1^2 \mathcal{K}_{0,1}' \end{vmatrix} = 0, \tag{35}$$

$$\mathcal{D}_4(\kappa_1, \kappa_2) \equiv \begin{vmatrix} (1 + \kappa_1^2)\mathcal{J}_{4,1} & (1 + \kappa_2^2)\mathcal{J}_{4,2} & 0 \\ \mathcal{J}_{4,1} & \mathcal{J}_{4,2} & \mathcal{K}_{4,1} \\ \left(1 + \frac{L_z}{L_\perp}\frac{1+\kappa_1^2}{F_1^{in}}\right)\mathcal{J}_{4,1} & \left(1 + \frac{L_z}{L_\perp}\frac{1+\kappa_2^2}{F_1^{in}}\right)\mathcal{J}_{4,2} & \mathcal{K}_{4,1}' \end{vmatrix} = 0, \tag{36}$$

where

$$c = \frac{F_1^{in}}{\kappa_1^2 \kappa_2^2}\left[F_1^{in} + \frac{L_\perp}{L_z} - \left(F_1^{in} + \frac{L_z}{L_\perp}\right)\frac{r_0^2}{4}\right] - 1,$$

$$d = -\frac{F_1^{in}}{\kappa_1^2 \kappa_2^2}\left(F_1^{in} + \frac{L_\perp}{L_z}\right)\frac{1 - \rho_1^2}{\rho_1^2} - 1. \tag{37}$$

Other notations are $\mathcal{J}_{i,j} = J_i(\kappa_j r_0)$ and $\mathcal{K}_{i,j} = K_i(\rho_j r_0)$, while the primes denote derivatives with respect to r_0.

A typical octupole is shown in Figs. 1 and 2. We adopted the background magnetic field parameters as $L_\perp = 1$, $L_z = 0.9 r_0$, and $s = 2.5/r_0^2$, with the core radius $r_0 = 0.1$. Thus, the vortex size is $\sim 10\%$ of the collisionless skin depth d_e, which is comparable with the beam radii of the devices described in [6,7]. This kind of structure is expected to emerge as the result of saturation of fast magnetic reconnection in the complex geometry of the accelerator's magnetic field which possesses an X line. The full dynamics of such a process is not studied here. It is expected to involve kinetic effects, such as the cyclotron damping of singular current layers, electron trapping, etc.

IV. CONCLUSIONS

We have shown that a high-intensity, relativistic electron beam that is in thermodynamic equilibrium can be properly described by the EMHD equations of plasma physics.

As the typical beam size in large machines is comparable to the electron collisionless skin depth, magnetic effects associated with the torsion of the flux tubes may develop in such systems. Most importantly, the complex magnetic geometry of the focusing magnetic field, possessing an X point at the beam axis, is unstable to fast magnetic reconnection. A plausible saturated state of the fast reconnection is presented, in the form of an octupolar vortex, which is characterized by a fully three-dimensional magnetic field perturbation. The nonlinear dispersion equations of the vortex have been derived and the relationship between the vortex structure and the background magnetic field has been discussed.

Our solution consists of localized octupoles, in both A_z and B_z, located at the original X point, which introduce a new

circular separatrix. As a consequence, new X points are created at the typical distance $\sim r_0$ from the original one. Such a multiplication of X points, resulting from the saturation of small-scale collisionless reconnection, provides a physically intriguing mechanism for introducing stochasticity into the beam.

ACKNOWLEDGMENTS

---

[1] R. C. Davidson, *Physics of Nonlinear Plasmas* (Addison-Wesley, Reading, MA, 1990).

[2] L. K. Spentzouris, J.-F. Ostiguy, and P. L. Colestock, Phys. Rev. Lett. **76**, 620 (1996).

[3] R. C. Davidson, B. H. Hui, and C. A. Kapetanakos, Phys. Fluids **18**, 104 (1975).

[4] M. Reiser, Phys. Fluids **20**, 477 (1977).

[5] S. M. Lund and R. C. Davidson, Phys. Plasmas **5**, 3028 (1998).

[6] B. Richter, in *Laser Acceleration of Particles*, edited by Chan Joshi and Thomas C. Katsouleas, AIP Conf. Proc. **130** (AIP, New York, 1985).

[7] A. G. A. Verhoveen, W. A. Bongers, W. L. Bratman, M. Caplan, G. G. Denisov, G. van Dijk, C. A. van der Greer, P. Manintveld, A. J. Poelman, J. Pluygers, M. Yu. Shmelyov, P. H. M. Smeets, A. B. Sterk, and W. H. Urbanus, Phys. Plasmas **5**, 2029 (1998).

[8] B. W. Church and R. N. Sudan, Phys. Plasmas **3**, 3809 (1996).

[9] R. C. Davidson, Phys. Plasmas **5**, 3459 (1998).

[10] A. S. Kingsep, K. V. Chukbar, and V. V. Yan'kov, Rev. Plasma Phys. **16**, 243 (1990).

[11] P. K. Shukla and L. Stenflo, Phys. Lett. A **259**, 49 (1999).

[12] S. V. Bulanov, S. G. Shasharina, and F. Pegoraro, Plasma Phys. Controlled Fusion **32**, 377 (1990).

[13] S. V. Bulanov, S. G. Shasharina, and F. Pegoraro, Plasma Phys. Controlled Fusion **34**, 33 (1991).

[14] S. V. Bulanov, F. Pegoraro, and A. S. Sakharov, Phys. Fluids B **4**, 2499 (1992).

[15] K. Avinash, S. V. Bulanov, T. Esirkepov, P. Kaw, F. Pegoraro, P. V. Sasorov, and A. Sen, Phys. Plasmas **5**, 2849 (1998).

[16] D. Jovanović, F. Pegoraro, and J. Juul Rasmussen, J. Plasma Phys. **60**, 383 (1998).

[17] J. Vranješ, D. Jovanović, and P. K. Shukla, Phys. Plasmas **5**, 4300 (1998).

[18] D. Jovanović and F. Pegoraro, Phys. Plasmas **7**, 889 (2000).